PHYSICSAccess Research Paper
ISSN Online: 2756-3898, ISSN Print: 2714-500X https://doi.org/10.47514/phyaccess.2026.6.1.009

Effect of Deposition Time on the Optoelectronic Properties of CdS Thin Films Synthesized via Chemical Bath Deposition Technique

Simon Ja'afaru[1,2], Isaac H Daniel[2], Yakubu A Tanko[2], Nicodemus Kure[2], and Olayinka A Babalola[1]

[1] Physics Advanced Research Centre, Sheda Science and Technology Complex (SHESTCO), Abuja, Nigeria
[2] Department of Physics, Kaduna State University, Kaduna, Kaduna State, Nigeria

Corresponding E-mail: simonjaf@gmail.com

Received 13-02-2026
Accepted for publication 25-03-2026
Published 27-03-2026

Abstract

Cadmium sulphide (CdS) thin films were synthesized via chemical bath deposition (CBD) to investigate the influence of deposition time on their optoelectronic properties. The films were deposited at 80 °C for durations ranging from 5 to 30 minutes. Film thickness increased from 1.5 to 3.0 µm with increasing deposition time, while surface roughness exhibited a non-linear variation associated with nucleation, growth, and grain agglomeration processes. X-ray diffraction of the 30-minute film confirmed a polycrystalline hexagonal CdS structure. Optical analysis revealed a non-linear variation in the bandgap, decreasing from 2.42 eV to 2.07 eV, with strong absorption in the visible region and a maximum absorption at 25 minutes. The refractive index, dielectric constants, and optical conductivity also varied with deposition time, indicating changes in optical response and carrier transport. Hall effect measurements confirmed n-type conductivity, with mobility increasing up to 25 minutes before decreasing, while carrier concentration and resistivity exhibited deposition-time dependence. The 20-minute film had a good mix of optical, electrical, and surface properties. The 30-minute film, on the other hand, had the highest photosensitivity (3110.08%) and responsivity (1.76×10^{-2} $mA.W^{-1}$). These findings indicate that deposition time is an essential factor for optimizing the optoelectronic performance of CdS thin films for photodetector applications.

Keywords: Cadmium Sulphide; Chemical Bath Deposition; Deposition Time; Optoelectronic Properties; Photosensitivity.

I. Introduction

Cadmium sulphide (CdS) is a II–VI semiconductor with a direct bandgap of approximately 2.4 eV, enabling effective absorption of visible light [1–4]. It exhibits n-type conductivity [5], a high absorption coefficient [6], and notable photoconductivity [7], making it suitable for optoelectronic applications. CdS thin films have been widely employed in devices such as solar cells, light-emitting diodes, and photodetectors [1], [8-9]. The combination of favorable electronic and optical properties, together with relatively simple synthesis, makes CdS an attractive material for both research and technological applications.

Various techniques have been employed for the synthesis of CdS thin films, including spin coating [10], spray pyrolysis [11], chemical bath deposition (CBD) [12-13], co-precipitation [14], successive ionic layer adsorption and reaction [3], and pulsed laser deposition [15]. These techniques differ in terms of equipment requirements, growth

conditions, cost, and the quality of films produced.

Chemical bath deposition (CBD) was employed in this study because it is a simple and cost-effective technique for producing CdS thin films [12-13], [16-18]. It operates at low temperatures, making it compatible with temperature-sensitive substrates, and enables uniform, adherent coatings over large areas without the need for vacuum systems [18]. By adjusting bath conditions, CBD allows precise control over film thickness and composition [16]. These advantages, combined with its scalability and energy efficiency [17], make CBD a versatile approach for both laboratory research and industrial production of semiconductor thin films.

Among the growth parameters in CBD, deposition time has a critical effect on nucleation rate, film thickness, grain growth, and defect density [19]. These structural factors strongly influence optical absorption, carrier transport, and photoconductive response [20]. Optimizing deposition time is therefore essential for achieving CdS thin films with enhanced optical, electrical, and photosensing performance, which are keys for high-performance optoelectronic devices [21].

Previous studies on deposition time effects in CdS thin films primarily focus on structural evolution and bandgap changes. However, limited attention has been given to dielectric properties, optical conductivity, and overall photodetector performance [20-25]. Addressing these parameters is necessary to provide a more comprehensive understanding of how deposition time influences the functional properties of CdS thin films.

In this work, CdS thin films deposited at 80 °C over a controlled time range (5–30 min) were comprehensively analyzed through surface profiling, optical dispersion parameters (extinction coefficient, refractive index, real and imaginary dielectric constants), optical conductivity, Hall effect measurements, and solar-simulator-based I–V characterization. This comprehensive analysis enables the identification of the optimal deposition time for achieving improved optoelectronic and photodetector performance.

II. Experiment

CdS thin films were synthesized through the chemical bath deposition (CBD) method. Solutions containing cadmium chloride ($CdCl_2$), thiourea (H_2NCSNH_2), and disodium EDTA ($Na_4(C_{10}H_{16}N_2O_8)$) were prepared at a concentration of 0.08 M in 50 mL of deionized water. The pH was adjusted to 10 using a 25% ammonium hydroxide (NH_4OH) solution. Initially, a 0.08 M $CdCl_2$ solution was treated with NH_4OH until a white precipitate of $Cd(OH)_2$ formed, which dissolved with additional NH_4OH. Afterward, 10 mL of 0.08 M EDTA and 50 mL of 0.08 M thiourea were added in sequence and mixed to begin the formation of CdS.

Glass slides, which served as substrates, were immersed in acetone, rinsed with deionized water, and then dried. The CdS solution was heated on a hot plate, and the substrates were immersed at room temperature. The temperature was gradually raised to 80 °C, after which the deposition time was recorded. Films were deposited for 5, 10, 15, 20, 25, and 30 minutes, then removed, rinsed with deionized water, and air-dried.

Following the identification of the 30-minute film with superior photosensitivity and responsivity, the sample was annealed at 200 °C for 30 minutes only for XRD analysis to improve crystallinity and phase identification. SEM characterization was performed on the unannealed film, and annealing was not considered as a variable in the deposition-time study.

Electrical contacts were achieved by applying conductive paste, prepared from graphite and nail hardener, on the CdS films to provide stable ohmic contacts for Current - Voltage (I-V) characterization.

A. Chemical Reactions and Mechanisms in the Synthesis of CdS Thin Film

1) Cadmium Chloride ($CdCl_2$) Dissociation

$CdCl_2$ dissociates in water to release cadmium ions (Cd^{2+}) and chloride ions (Cl^-).

$$CdCl_2 \rightarrow Cd^{2+} + 2Cl^- \quad (1)$$

2) Thiourea (H_2NCSNH_2) Decomposition

Thiourea decomposes in the presence of ammonia (NH_4OH) when heated, releasing sulfur ions (S^{2-}).

$$H_2NCSNH_2 + 2OH^- \rightarrow S^{2-} + CN_2H_2 + 2H_2O \quad (2)$$

3) Formation of Cadmium Sulfide (CdS)

Cadmium ions (Cd^{2+}) from cadmium chloride react with sulfide ions (S^{2-}) from thiourea to form cadmium sulphide (CdS), which deposits as a thin film on the substrate:

$$Cd^{2+} + S^{2-} \rightarrow CdS\ (\text{thin film}) \quad (3)$$

The thickness of the film and its surface roughness were assessed utilizing a Veeco Dektak 150 stylus profiler.

Optical characteristics such as absorbance and transmittance were evaluated with a UV–Vis spectrophotometer (Filmetrics F10–RT) across a wavelength range of 250–1100 nm. The optical parameters, absorption coefficient, optical band gap, refractive index, extinction coefficient, real and imaginary dielectric constant, and optical conductivity, were computed using (4), (5), (6), (7), (8), (9), and (10), respectively.

$$\alpha = \frac{\ln(1/T)}{t} \quad (4)$$

$$(\alpha h\upsilon)^2 = A\left(h\upsilon - E_g\right) \quad (5)$$

$$\eta = \frac{1+\sqrt{R}}{1-\sqrt{R}} \quad (6)$$

$$k = \frac{\alpha\lambda}{4\pi} \quad (7)$$

$$\varepsilon_r = \eta^2 - k^2 \quad (8)$$

$$\varepsilon_i = 2\eta k \quad (9)$$

$$\sigma = \frac{\alpha\eta c}{4\pi} \quad (10)$$

Where T is the transmittance, t is the film thickness, λ is the wavelength of incident light, $h\upsilon$ is the photon energy, R is the reflectance, and c is the speed of light [26-31].

The electrical properties, which include carrier concentration, mobility, resistivity and average hall coefficient, were analyzed using an ECOPIA Hall Effect Measurement System (HMS-3000) at 300 K. The current–voltage (I–V) characterization was carried out using a Keithley 2400 SourceMeter under illumination from a Newport Oriel Solar Simulator operating at AM 1.5G with an intensity of 100 mW.cm^{-2} and a wavelength range of 300–1400 nm. This was conducted under dark and illumination to determine photosensitivity and responsivity, using (11) and (12).

$$S(\%) = \frac{I_{Light} - I_{Dark}}{I_{Dark}} \times 100 \quad (11)$$

$$R = \frac{I_{ph}(A)}{E(W/c^{2})\,A(cm^{2})} = \frac{I_{ph}(A)}{P_{inc}(W)} \quad (12)$$

Where I_{Light} *and* I_{Dark} denote the photocurrent and dark current, respectively, and P_{inc} is the incident optical power [9].

The crystal structure and phase composition of the 30-minute film were examined using a Tonda TD–3500 X-ray diffractometer equipped with CuKα radiation (λ = 1.5406 Å).

Structural parameters, crystallite size, dislocation density, and microstrain were derived using (13), (14), and (15).

$$D = \frac{K\lambda}{\beta cos\Theta} \quad (13)$$

$$\rho = \frac{1}{D^{2}} \quad (14)$$

$$\epsilon = \frac{\beta}{4tan\theta} \quad (15)$$

Where K is the Scherrer constant, β is the FWHM, and θ is the Bragg angle [32-34].

The surface morphology was scrutinized using a ZEISS EVO MA 10 Scanning Electron Microscope (SEM).

III. RESULTS AND DISCUSSION

A. Surface Profiling for Thickness and Surface Roughness

Fig. 1 presents the surface profiles of CdS thin films deposited at 80 °C for different durations: (a) 5 minutes, (b) 10 minutes, (c) 15 minutes, (d) 20 minutes, (e) 25 minutes, and (f) 30 minutes.

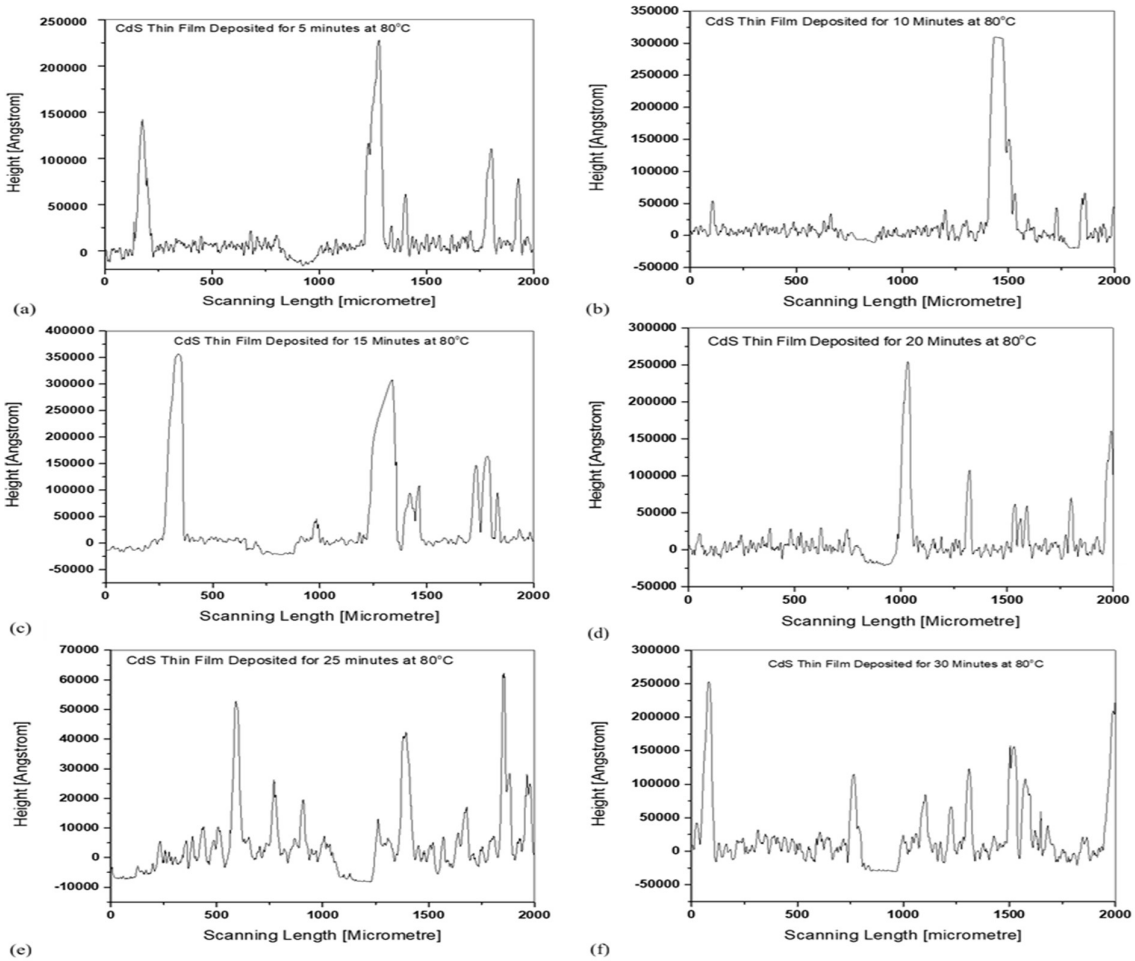

Fig. 1. Plot of surface profiles of CdS samples deposited for variable deposition times at 80 °C.

The profiles provide insight into the evolution of film thickness and surface morphology during growth. At shorter deposition times, 5–10 minutes (see Fig.1(a) and (b)), the profiles appear relatively shallow and less defined,

corresponding to the initial nucleation stage where isolated CdS clusters begin to form on the substrate. As the deposition time increases to 15 and 20 minutes (see Fig. 1(c) and (d)), the profiles become more pronounced, reflecting continuous film growth and increased thickness due to sustained precipitation of CdS.

At 25 minutes (see Fig. 1(e)), the profile exhibits a noticeable reduction in depth, consistent with the decrease in measured thickness. This behaviour suggests the onset of dissolution or desorption processes within the chemical bath, leading to partial removal of previously deposited material. At 30 minutes (see Fig. 1(f)), the profile becomes significantly deeper and more defined, indicating renewed film growth and the formation of a thicker layer. This evolution of surface profiles highlights the dynamic nature of the deposition process, governed by the interplay between film growth and dissolution mechanisms.

The minimum height extracted from each surface profile was taken as the film thickness, and the corresponding values for all samples are presented in Table I.

Table I. Thickness and average roughness of CdS samples deposited for variable times at 80 °C derived from the surface profiles.

Deposition Time (minutes)	Thickness D (μm)	Average Roughness Ra (nm)
5.0	1.5	1325.44
10	1.9	2628.70
15	2.0	5484.70
20	2.1	1994.60
25	0.8	699.70
30	3.0	3029.70

Fig. 2, together with Table I, shows the variation of film thickness with deposition time. The thickness increases from 1.5 μm at 5 minutes to 2.1 μm at 20 minutes, which can be attributed to sustained nucleation and growth of CdS on the substrate due to the continuous release of Cd^{2+} and S^{2-} ions in the bath. During this stage, the deposition process dominates, resulting in progressive film thickening.

The observed decrease in film thickness at 25 minutes can be attributed to the interplay between two competing processes inherent to chemical bath deposition: (i) heterogeneous and homogeneous precipitation of CdS, which drives film growth, and (ii) dissolution of the pre-formed CdS layer in the alkaline bath. At shorter deposition times, the concentration of reactive species is sufficiently high, and the growth process dominates, resulting in a progressive increase in film thickness. However, as deposition time increases, depletion of precursor ions reduces the rate of CdS formation, while dissolution and desorption processes become increasingly significant. This shift in dominance leads to a net reduction in film thickness. Similar behaviour has been reported for CBD-grown CdS thin films in the literature [35].

At 30 minutes, the thickness increases sharply to 3.0 μm, which may be attributed to a renewed dominance of the deposition process, possibly due to secondary nucleation or changes in bath chemistry that enhance CdS formation. This non-linear behaviour highlights the complex growth dynamics of CdS thin films in chemical bath deposition.

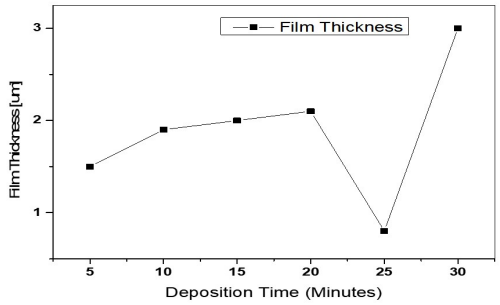

Fig. 2. Plot of CdS samples' thickness against deposition time.

At 30 minutes, the roughness increases again to 3,029.70 nm, which is likely attributed to grain agglomeration and clustering effects. The formation of larger surface features and the coalescence of grains introduce surface irregularities, resulting in increased roughness, consistent with reports in the literature [37]. It is important to note that these larger surface features do not necessarily correspond to larger crystallite sizes, as X-ray diffraction analysis suggests a relatively smaller crystallite size at this deposition time. This indicates that the film may consist of agglomerated structures composed of smaller coherent crystallite domains, possibly due to structural reorganization during prolonged deposition. This trend reflects the evolution of film growth from nucleation-dominated to coalescence and eventual agglomeration stages.

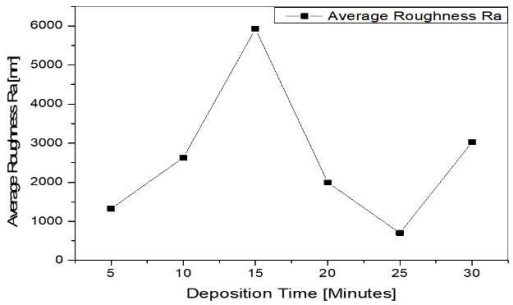

Fig. 3. Plot of CdS samples' average roughness ra against deposition time.

B. Optical Characterization

The optical properties of the CdS thin films are strongly influenced by the deposition time, as evidenced in Fig. 4. The absorbance spectra shown in Fig. 4(a) indicate a general decrease with increasing wavelength, with stronger absorption in the visible region and weaker absorption in the near-infrared (NIR). The film deposited for 15 minutes exhibits the highest absorbance in the visible range, reflecting effective photon capture at this deposition time, while the 30-minute film shows the highest absorbance in the NIR region, likely due to increased thickness and enhanced light scattering at the

surface. The 25-minute film also displays relatively high absorbance, suggesting improved surface uniformity and density that promote photon interaction.

The transmittance spectra in Fig. 4(b) show an inverse trend relative to absorbance. Films deposited for 20 and 25 minutes exhibit the highest transparency in the visible range, whereas the 30-minute film shows the lowest transmittance, consistent with its increased thickness and denser microstructure. The 15-minute film presents moderate transmittance, indicating that although thinner films allow more light passage, insufficient thickness can reduce uniformity and partially limit optical transmission. These observations highlight the dependence of optical transparency on both film thickness and surface morphology.

The absorption coefficient, illustrated in Fig. 4(c), follows a pattern similar to absorbance, with higher values observed at shorter wavelengths. The 25-minute film reaches the maximum absorption coefficient, indicating enhanced photon absorption and optical response, likely due to optimized thickness, grain growth, and reduced defect scattering. In comparison, the 15- and 20-minute films show slightly lower absorption, while the 30-minute film, despite its greater thickness, exhibits reduced absorption in the visible region, which may result from structural inhomogeneity at extended deposition times.

The optical bandgap derived from Tauc plots (Fig. 4(d)) decreases non-linearly from 2.42 eV at 5 minutes to 2.32 eV at 15 minutes, with minor fluctuations before reaching 2.07 eV at 30 minutes. This reduction is attributed to increased film thickness and grain growth, which reduce quantum confinement effects, while band tailing caused by defect states and improved crystallinity at longer deposition times further contribute to bandgap narrowing. The slight fluctuations observed at intermediate deposition times reflect variations in surface roughness and microstructure, in agreement with the trends in absorbance and transmittance.

Collectively, these results demonstrate that deposition time has a significant impact on the optical behaviour of CdS thin films. Short deposition times (5–15 minutes) favour high visible absorbance but moderate transparency, whereas moderate times (20–25 minutes) optimize both transmittance and absorption coefficient. Longer deposition (30 minutes) shifts absorption toward longer wavelengths but reduces overall transparency, likely due to increased surface roughness and non-uniformity. Overall, a deposition time of 25 minutes appears optimal for achieving high optical absorption while maintaining reasonable transparency, indicating the importance of carefully controlling deposition duration to tailor the optical properties of CdS thin films.

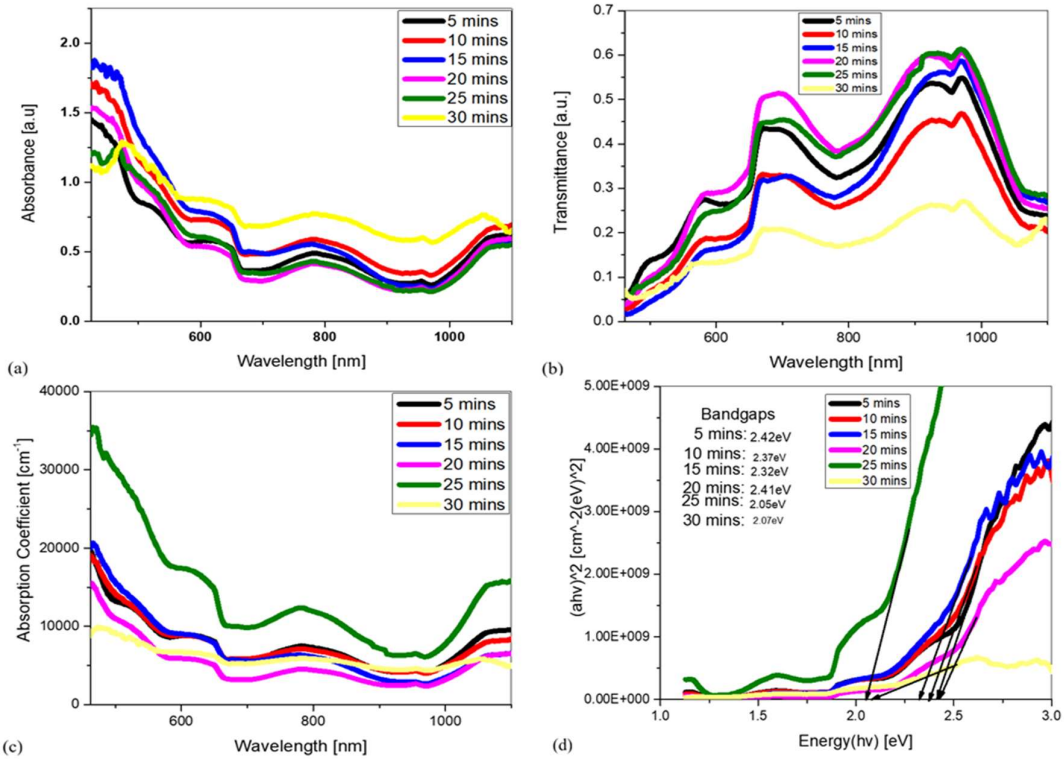

Fig. 4. Plots of (a) Absorbance, (b) Transmittance, (c) Absorption Coefficient, and (d) $(\alpha h\upsilon)^2$ Vs energy $(h\upsilon)$ for bandgaps.

Fig. 5 presents the variation of optical constants with wavelength for CdS thin films deposited at different times. The extinction coefficient (Fig. 5(a)) exhibits a significant increase in the UV region for all samples, indicating strong photon absorption characteristic of CdS. In the visible region, the film deposited for 25 minutes shows the highest peak value

of 0.1325 cm^{-1}, while the 30-minute film exhibits the lowest absorption, suggesting a reduction in optical absorption with prolonged deposition time.

The refractive index (Fig. 5(b)) increases across the visible to NIR region, reaching a maximum value of approximately 3.00 for the 30-minute film, whereas the other samples remain around 2.64. This behaviour indicates a dependence on film thickness and possible structural variations at longer deposition times.

The real dielectric constant (Fig. 5(c)) follows a similar trend, increasing to about 7 for most films, while the 30-minute sample shows lower values in the range of approximately 2–5.5. This reduction may be attributed to increased surface roughness and structural irregularities, which affect the material's polarization response.

The imaginary dielectric constant (Fig. 5(d)) varies with deposition time and wavelength, with the film deposited at 25 minutes exhibiting the highest values of 0.40 in the visible region and 0.66 in the NIR region, indicating increased optical energy loss. In contrast, the 5-minute film shows values of 0.24 and 0.37, while the 30-minute film exhibits the lowest values of 0.13 and 0.18. Notably, all values remain below unity, reflecting moderate absorption losses.

The optical conductivity (Fig. 5(e)) also shows a dependence on deposition time, with values reaching 1.14×10^{10} s^{-1} for the 5-minute film and peaking at 2.07×10^{10} s^{-1} for the 25-minute film, followed by a decrease at longer deposition times. This trend suggests that film thickness and microstructural evolution influence charge carrier excitation and transport within the films.

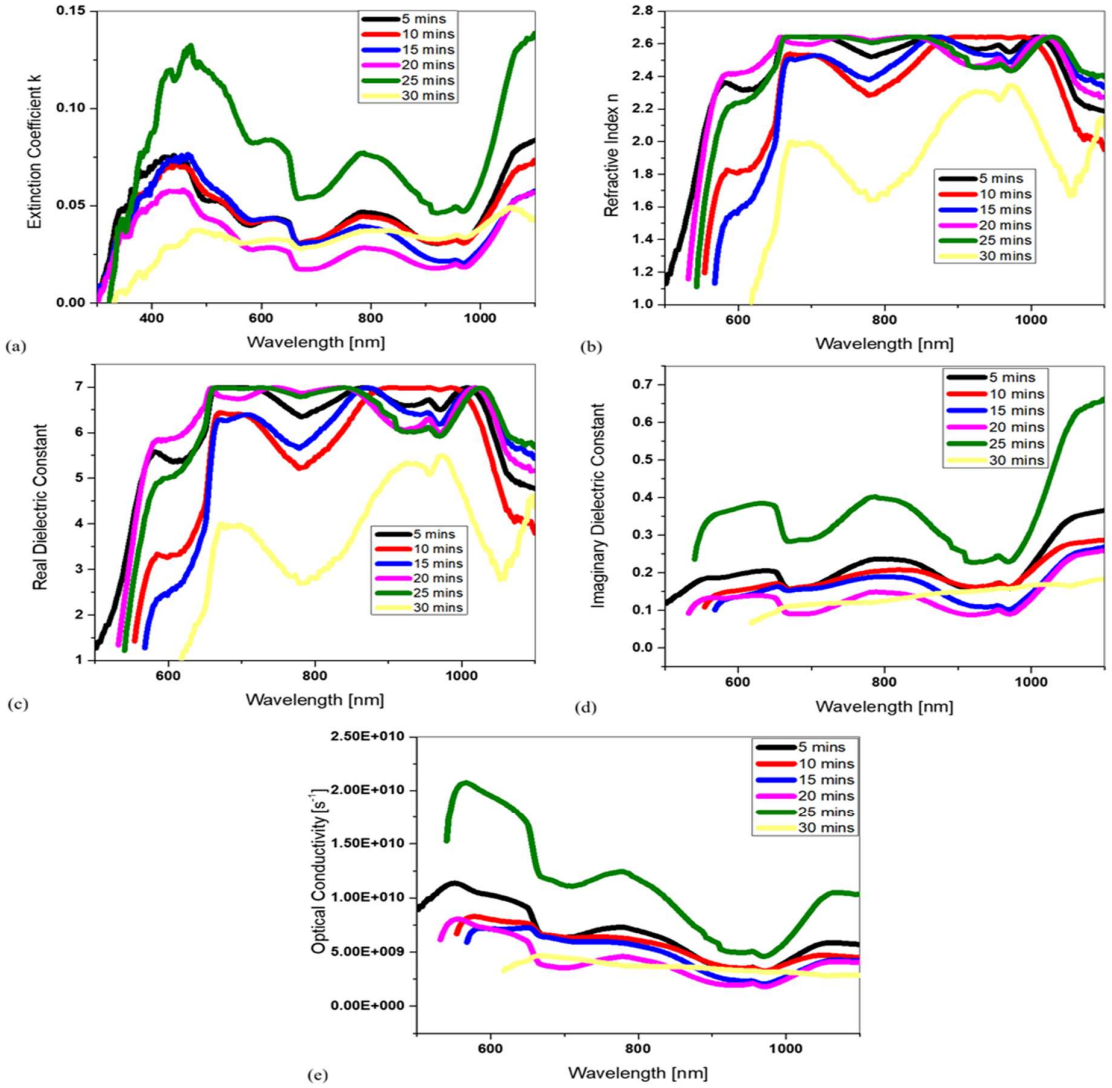

Fig. 5. Plots of (a) Extinction coefficient, (b) refractive index, (c) real dielectric constant, (d) Imaginary dielectric constant, and (e) Optical conductivity of CdS thin films.

C. Electrical Properties from Hall Effect Measurement

The Hall Effect measurement data, which includes bulk concentration, Hall mobility, resistivity, and the Hall coefficient for CdS thin films deposited at different times, provide insight into the electrical properties of these films.

As shown in Table II, the carrier concentration grows during the initial 10 minutes, begins to decrease with extended deposition times, reaching a minimum at 25 minutes, which aligns with the observed decrease in film thickness. Hall mobility increases consistently up to 25 minutes, suggesting improved charge transport and reduced scattering, but drops at 30 minutes, likely due to grain boundary effects. Initially, resistivity decreases, reflecting increased conductivity up to 15 minutes, but then rises after 20 minutes, possibly reflecting reduced film quality. The Hall coefficient becomes more negative with longer deposition times, consistent with the prevailing n-type conductivity and a decrease in carrier density with extended deposition durations.

Table II. Hall Effect Measurement Results of CdS Samples Deposited for Variable Times at 80 °C.

Deposition Time Variation (minutes)	Bulk Concentration (cm^{-3})	Hall Mobility ($cm^2.Vs^{-1}$)	Resistivity (Ωcm)	Average Hall Coefficient ($cm^3.C^{-1}$)
5.0	-9.759E+11	1.866E+02	3.427E+04	-6.396E+06
10.0	-4.436E+12	2.096E+02	6.715E+03	-1.407E+06
15.0	-2.964E+12	5.444E+02	3.869E+03	-2.106E+06
20.0	-4.046E+11	3.373E+02	4.574E+04	-1.543E+07
25.0	-5.593E+10	1.420E+03	7.862E+04	-1.068E+08
30.0	-2.662E+11	3.539E+02	6.625E+04	-2.345E+07

D. Current – Voltage (I-V) Characterization

Fig. 6 presents the current–voltage (I–V) characteristics of CdS thin films deposited for different durations under dark and illuminated conditions. For all samples, the current increases with applied voltage, with significantly higher current observed under illumination compared to dark conditions, confirming the photoconductive nature of the films.

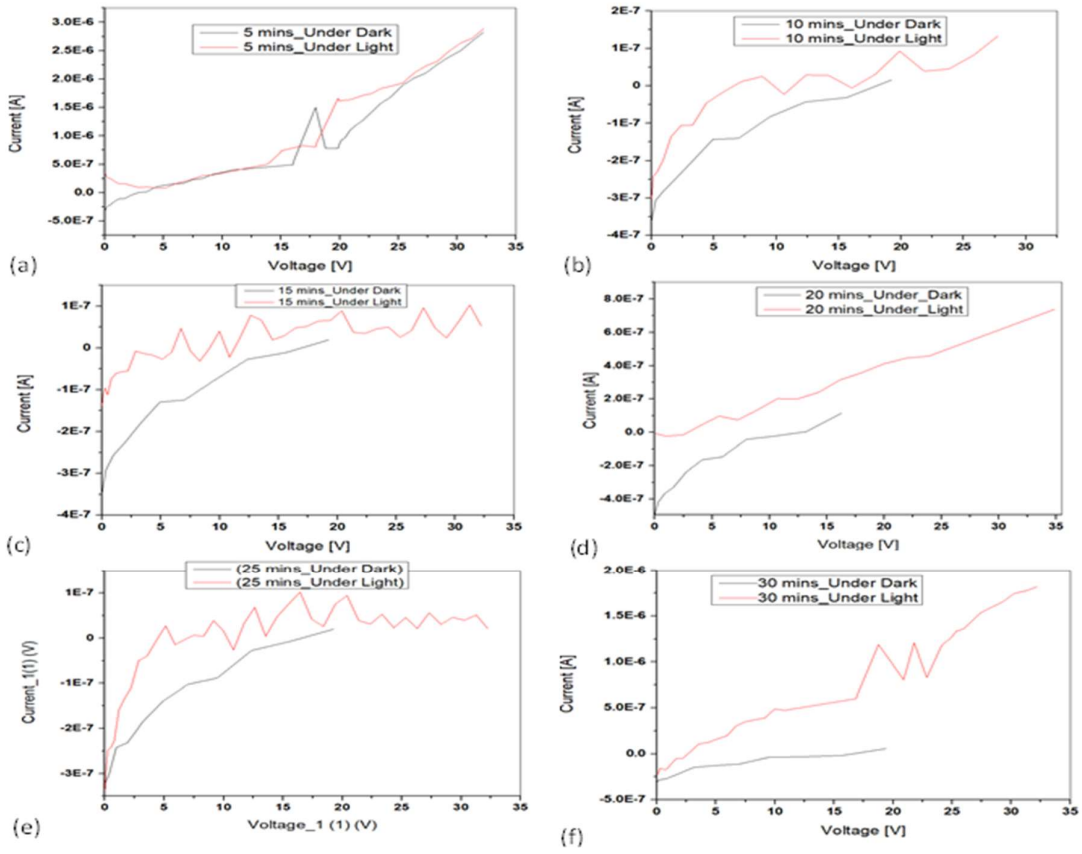

Fig. 6. Plots of I-V Curves (under Dark and Light Conditions) of CdS Samples deposited for variable Deposition Times at 80 °C.

For the 5-minute film (Fig. 6(a)), the current increases gradually with voltage, with a noticeable enhancement under illumination, although slight fluctuations are observed at intermediate voltages. The 10-minute film (Fig. 6(b)) shows improved photocurrent response with a more stable increase in current under light, indicating enhanced charge carrier generation compared to the 5-minute sample.

In the case of the 15-minute film (Fig. 6(c)), the photocurrent exhibits more pronounced fluctuations, which may be attributed to trap-assisted recombination or structural

inhomogeneities affecting carrier transport. The 20-minute film (Fig. 6(d)) demonstrates a more uniform and steady increase in current under illumination, suggesting improved film quality and more efficient charge transport mechanisms.

The 25-minute film (Fig. 6(e)) shows a strong photocurrent response, with a clear separation between dark and illuminated currents, indicating enhanced photoconductivity. The improved performance at this deposition time may be attributed to an optimal film thickness and microstructure, which facilitate the efficient generation and transport of charge carriers.

The 30-minute film (Fig. 6(f)) exhibits the highest photocurrent among all samples, with a significant increase in current under illumination. However, the presence of fluctuations at higher voltages suggests the presence of increased defect states or recombination processes at longer deposition times. Overall, the observed trends indicate that deposition time strongly influences the electrical and photoconductive behaviour of CdS thin films, with intermediate deposition times providing more stable transport characteristics, while longer deposition times enhance sensitivity.

In Fig. 7 and 8, the photosensitivity and responsivity of the CdS thin films exhibit distinct trends across various deposition times. At 5 minutes, the low photosensitivity (2.08%) and responsivity ($5.89 \times 10^{-4}\,\mathrm{mA.W^{-1}}$) indicate relatively poor photodetector performance, which may be related to a high dark current approaching the light current. This behavior may result from surface defects, suggesting that this deposition time may not be optimal for photodetection.

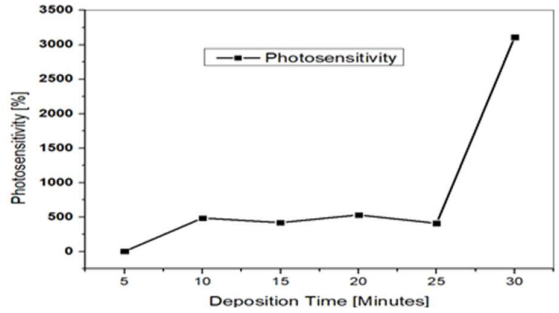

Fig. 7. A Plot of Photosensitivity of CdS Samples against Deposition Time.

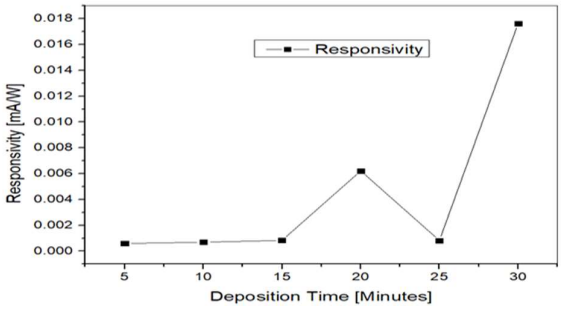

Fig. 8. A Plot of Responsivity of CdS Samples against Deposition Time.

As the deposition time increases to 10 and 15 minutes, there is a marked improvement in both photosensitivity (486.01% and 420.06%, respectively) and responsivity (6.95×10^{-4} $\mathrm{mA.W^{-1}}$ and 8.32×10^{-4} $\mathrm{mA.W^{-1}}$). This trend suggests an enhanced ability of the films to distinguish between light and dark conditions, which may be associated with reduced dark current and increased photocurrent generation. These results indicate that the films exhibit improved photodetection performance at these deposition times, although the performance may not yet be optimal.

The films deposited for 20 and 30 minutes exhibit the highest performance among the samples studied, with photosensitivity peaking at 3110.08% and responsivity reaching $1.76 \times 10^{-2}\,\mathrm{mA.W^{-1}}$ for the 30-minute sample, while the 20-minute film shows relatively balanced performance with good sensitivity and conversion efficiency (photosensitivity: 531.35%, responsivity: $6.22 \times 10^{-3}\,\mathrm{mA.W^{-1}}$). The 30-minute sample exhibits higher photosensitivity and responsivity, but with a slight increase in dark current. Thus, the 20-minute deposition time appears to provide a more balanced photodetection performance, whereas the 30-minute sample may be more suitable for applications requiring high sensitivity. For the 25-minute deposition, a responsivity of $8.0 \times 10^{-4}\,\mathrm{mA.W^{-1}}$ and a photosensitivity of 410% were recorded.

E. Structural Analysis

Fig. 9 shows the XRD spectra of a 30-minute deposition-time CdS thin film annealed at 200 °C. The film appears to be polycrystalline with a hexagonal structure, exhibiting prominent peaks at 24.92° (100), 26.48° (002), and 28.30° (101), consistent with JCPDS card no. 96-900-8863.

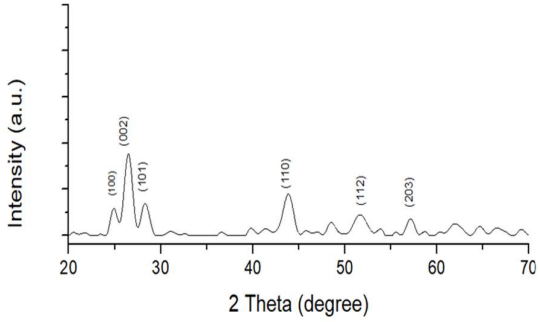

Fig. 9. XRD Plot for 30-minute deposition time CdS thin film annealed at 200 ℃.

As shown in Table III, the 30-minute CdS thin film annealed at 200 °C exhibits a relatively small crystallite size of 9.04 nm, indicating a nanocrystalline structure. While smaller crystallite sizes are typically associated with higher defect density, the relatively low dislocation density and microstrain values observed here suggest that annealing may have facilitated defect relaxation and structural reorganization. This results in improved crystalline quality despite the reduced crystallite size.

Table III. Microstructure properties of 30-minute CdS thin film (annealed at 200 ℃).

Sample	Crystallite Size $D = \frac{K\lambda}{\beta\cos\theta}$ (nm)	Dislocation Density $\rho = \frac{1}{D^2}$ (nm^{-2})	Microstrain $\epsilon = \frac{\beta}{4\tan\theta}$
30-minute CdS (annealed at 200 ℃)	9.04	0.0122	0.0127

F. Morphological Characteristics

The SEM image (Fig. 10) shows a granular and compact surface texture composed of very fine grains. The slightly non-uniform brightness indicates minor variations in grain orientation, suggesting an early stage of crystallization. No visible voids or cracks are observed, indicating good substrate coverage.

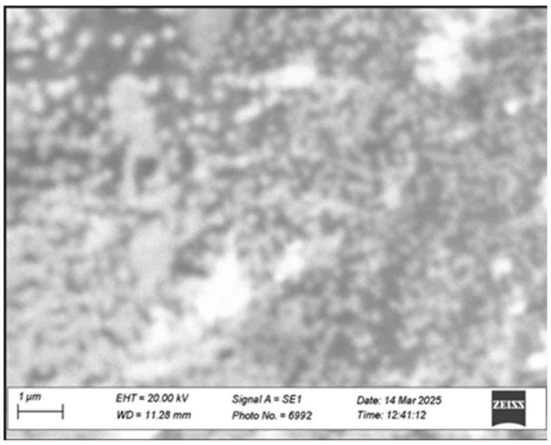

Fig. 10. SEM image of CdS Thin Film (30-minute deposition time).

IV. CONCLUSION

Deposition time has a notable effect on the optical and electrical properties of CdS thin films. Longer deposition times tend to increase film thickness and light absorption, but may also introduce surface irregularities and higher dark currents. Among the samples studied, the 20-minute film shows a relatively balanced combination of electrical conductivity, surface quality, and photosensing performance. It provides a favourable balance between responsivity, photosensitivity, and dark current levels, suggesting its suitability as a base layer for further modifications such as doping.

Reference

[1] D. Yi, J. Yang, R. Yang, K. Shen, D. Wang, and D. Wang, "Cu-doped CdS and its application in CdTe thin film solar cell," *AIP Advances*, vol. 6, no.1, 015203, 2016.

[2] Y. Chen, F. Wang, H. Xu, S. Ren, H. Gu, L. Wu, and L. Feng, "Properties of indium-doped CdS thin films and their photovoltaic application in CdTe solar cells," *Chalcogenide Letters*, vol. 14, no. 1, 2017.

[3] P. R. Ghediya, T. K. Chaudhuri, J. Ray, H. L. Panjwani, P. J. Hemani, P. P. Paneri, and R. R. Joshi, "Synthesis and characterizations of copper cadmium sulphide ($CuCdS_2$) as a potential absorber for thin film photovoltaics," *Materials Chemistry and Physics*, vol. 252, 123382, 2020, doi: 10.1016/j.matchemphys.

[4] A. Z. Thoalfiqar, A. A. Noora, J. Ali, H. A. Khalid, F. H. Nadir, and S. C. Sami, "Synthesis of nanocrystalline cadmium sulphide film and the influence of Cu doping on the physical characterization," *Journal of Nanostructures*, vol. 11, no. 2, pp. 269–275, 2021.

[5] K. Yilmaz, "Some structural, electrical, and optical properties of vacuum evaporated CdS thin films," *Journal of Ovonic Research*, vol. 10, pp. 211–219, 2014.

[6] J. Hakami, "Highly induced photosensing behavior of Erbium (Er), Yttrium (Y) and Terbium (Tb) doped nanostructured cadmium sulphide (CdS) thin films prepared by nebulizer spray pyrolysis method," *Journal of Alloys and Compounds*, vol. 924, 166577, 2022.

[7] S. Majumder, P. K. Baviskar, and B. R. Sankapal, "Straightening of chemically deposited CdS nanowires through annealing towards improved PV device performance," *Ceramics International*, vol. 42, no. 6, pp. 6682–6691, 2016.

[8] T. T. Xuan, J. Q. Liu, R. J. Xie, H. L. Li, and Z. Sun, "Microwave-assisted synthesis of CdS/ZnS:Cu quantum dots for white light-emitting diodes with high color rendition," *Chemistry of Materials*, vol. 27, no. 4, pp. 1187–1193, 2015.

[9] M. Husham and Z. Hassan, "Synthesis of nanocrystalline CdS thin films via microwave-assisted chemical bath deposition for highly photosensitive and rapid response photodetectors," *Journal of Nanoelectronics and Optoelectronics*, vol. 10, pp. 1–7, 2015.

[10] J. Sharma, M. Mishra, S. Jain, and B. Tripathi, "Tuning of structural, optical, and electrical characteristics of Cu/CdS composite thin films for energy applications," *International Journal of Advances in Engineering and Management*, vol. 4, pp. 507–517, 2022.

[11] T. Zaker, N. Aziz, A. Mohammed, H. Haneen, N. Fadhil, and S. Salman, "Synthesis of nanocrystalline cadmium sulphide film and the influence of Cu doping on the physical characterization," *Journal of Nanostructures*, vol. 11, pp. 269–275, 2021.

[12] R. Corral, R. Ochoa, A. Apolinar, and S. Castillo, "Optical and structural properties of ammonia-free CdS:Cu thin film grown on a flexible substrate by the chemical bath method," *Chalcogenide Letters*, vol. 15, pp. 429–434, 2018.

[13] S. Inthong, P. Intawin, A. Kraipok, J. Kanthachan, S. Eitssayeam, U. Inthata, S. Denis, and T. Tunkasiri, "Investigation of Cu-doped cadmium sulphide photoconductive cells," *Engineering Journal Chiang Mai Journal of Science*, vol. 46, no. 5, pp. 1009–1014, 2019.

[14] D. Pradhabhan and A. Sakthivelu, "Optical, structural and electrical properties of Cu-doped CdS thin films fabricated by SILAR method," *International Journal of Engineering Research and Technology*, vol. 8, pp. 623–627, 2019.

[15] S. Cai, X. Xu, W. Yang, J. Chen, and X. Fang, "Materials and designs for wearable photodetectors," *Advanced Materials*, vol. 31, no. 18, 1808138, 2019.

[16] H. Ali, "Advances in chemical bath deposition for metal chalcogenide thin films: A review," *Solar Energy Materials and Solar Cells*, vol. 246, 111904, 2022.

[17] G. M. Di Mari, V. La Matta, V. Strano, R. Reitano, P. Cerruti, G. Filippone, ... and E. Bruno, "Optimized chemical bath deposition for low cost, scalable, and environmentally sustainable synthesis of star-like ZnO nanostructures," *ACS Omega*, vol. 9, no. 37, pp. 38591–38598, 2024.

[18] F. T. Z. Toma, S. Rahman, K. M. A. Hussain, and S. Ahmed, "Thin film deposition techniques: A comprehensive review," *Journal of Modern Nanotechnology*, vol. 4, no. 6, 2024.

[19] A. Z. Arsad, A. W. M. Zuhdi, S. F. Abdullah, C. F. Chau, A. Ghazali, I. Ahmad, and W. S. W. Abdullah, "Effect of chemical bath deposition variables on the properties of zinc sulfide thin films: a review," *Molecules*, vol. 28, no. 6, 2780, 2023.

[20] M. Maghouli and H. Eshghi, "Effect of deposition time on physical properties of nanostructured CdS thin films grown by chemical bath deposition technique," *Superlattices and Microstructures*, vol. 128, pp. 327–333, 2019.

[21] A. El-Shaer, S. Ezzat, M. A. Habib, O. K. Alduaij, T. M. Meaz, and S. A. El-Attar, "Influence of deposition time on structural, morphological, and optical properties of CdS thin films grown by low-cost chemical bath deposition," *Crystals*, vol. 13, no. 5, 788, 2023.

[22] S. Hariech, J. Bougdira, M. Belmahi, G. Medjahdi, M. S. Aida, and A. Zertal, "Effect of deposition time on chemical bath deposited CdS thin films properties," *Bulletin of Materials Science*, vol. 45, no. 2, 78, 2022.

[23] A. Kumar, D. Pednekar, S. Mukherjee, and R. K. Choubey, "Effect of deposition time and complexing agents on hierarchical nanoflake-structured CdS thin films," *Journal of Materials Science: Materials in Electronics*, vol. 31, no. 19, pp. 17055–17066, 2020.

[24] O. K. Echendu, U. S. Mbamara, K. B. Okeoma, C. Iroegbu, C. A. Madu, I. C. Ndukwe, and I. M. Dharmadasa, "Effects of deposition time and post-deposition annealing on the physical and chemical properties of electrodeposited CdS thin films for solar cell application," *Journal of Materials Science: Materials in Electronics*, vol. 27, no. 10, pp. 10180–10191, 2016.

[25] K. H. Chol, C. H. Ho, K. Y. Jo, and S. G. Il, "Effect of the reactant concentration, bath temperature, and deposition time on the properties of CdS thin film prepared by the chemical bath deposition method," *Optical Materials*, vol. 112, 110790, 2021.

[26] I. E. Ottih, A. J. Ekpunobi, and P. I. Ekwo, "Solid state and optical properties of chemical bath deposited copper nickel sulphide (CuNiS) thin films," *The Pacific Journal of Science and Technology*, vol. 12, no. 2, pp. 342–347, 2011.

[27] M. T. Abdullah, L. M. Raoof, M. H. Hasan, A. N. Abd, and I. M. Mohammed, "The effect of different thickness on the optical and electrical properties of TiO_2 thin films," *Journal of Physics: Conference Series*, vol. 1999, no. 1, 012128, Sep. 2021, doi: 10.1088/1742-6596/1999/1/012128.

[28] J. Hirpara, G. Malik, and R. Chandra, "Optical properties investigation of reactively sputtered tantalum oxynitride films," *Materials Today: Proceedings*, vol. 57, pp. 202–210, 2022.

[29] R. Dutta, S. I. P. Tian, Z. Liu, M. Lakshminarayanan, S. Venkataraj, Y. Cheng, D. Bash, V. Chellappan, T. Buonassisi, and S. Jayavelu, "Extracting film thickness and optical constants from spectrophotometric data by evolutionary optimization," *PLoS ONE*, vol. 17, no. 11, e0276555, Nov. 2022, doi: 10.1371/journal.pone.0276555.

[30] J. Zhou, Y. Yang, and C. Y. Zhang, "Toward biocompatible semiconductor quantum dots: From biosynthesis and bioconjugation to biomedical application," *Chemical Reviews*, vol. 115, no. 21, pp. 11669–11717, 2015.

[31] B. Mahrov, G. Boschloo, A. Hgfeldi, L. Dloczuk, and T. Diffrich, "Photovoltaic study of charge injection from dye molecules into transparent hole and electron conductors," *Applied Physics Letters*, vol. 84, no. 26, pp. 5455–5457, 2004.

[32] A. L. Patterson, "The Scherrer formula for X-ray particle size determination," *Physical Review*, vol. 56, no. 10, pp. 978–982, 1939.

[33] D. K. Rawat and P. K. Shishodia, "Growth of ZnO thin films doped with (Mn & Co) by spin coating technique," in *AIP Conference Proceedings*, vol. 1728, no. 1, 020256, May 2016.

[34] A. S. Gadallah and M. M. El-Nahass, "Structural, optical constants and photoluminescence of ZnO thin films grown by sol-gel spin coating," *Advances in Condensed Matter Physics*, vol. 2013, 234546, 2013.

[35] F. Ouachtari, A. Rmili, B. Elidrissi, A. Bouaoud, H. Erguig, and P. Elies, "Influence of bath temperature, deposition time and S/Cd ratio on the structure, surface morphology, chemical composition and optical properties of CdS thin films elaborated by

chemical bath deposition," *Journal of Modern Physics*, vol. 2, no. 9, pp. 1073–1082, 2011.

[36] X. R. Chen, B. C. Zhao, C. Yan, and Q. Zhang, "Review on Li deposition in working batteries: From nucleation to early growth," *Advanced Materials*, vol. 33, no. 8, 2004128, 2021.

[37] J. P. Enríquez and X. Mathew, "Influence of the thickness on structural, optical and electrical properties of chemical bath deposited CdS thin films," *Solar Energy Materials and Solar Cells*, vol. 76, no. 3, pp. 313–322, 2003.